

# COLLISION AVOIDANCE USING THE LGMD MODEL MEAN RESPONSE

**Adriano Dídimo, Ana Carolina Vilares, Cristina Peixoto Santos**

*Industrial Electronics Department  
University of Minho  
Guimarães, Portugal*

**Abstract:** The Lobula Giant Movement Detector (LGMD) neuron, part of the locust optic lobe, responds selectively to rapidly approaching objects. In this article, we use a neural network that models the LGMD neuron. We propose a LGMD-based obstacles detection system to detect and avoid obstacles. In particular, we propose a new way to analyse the output of the LGMD model which decreases the complexity of the algorithm but increases the precision of the detection.

The system performance is verified in an experiment in which a mobile robot equipped with a camera on its top, must autonomously navigate in a simulated environment. The obtained results show the system robustness and reliability.

**Keywords:** Neural networks, Autonomous mobile robots, Bio robot control, Computer Vision

## 1. INTRODUCTION

Vision plays for a larger number of species a key role in survival. In robotics, many navigation methods are based on visual information. However, these systems are normally very costly computationally.

The Lobula Giant Movement Detector neuron (or LGMD), part of the locust's optic lobe, responds selectively to approaching objects (Rind and Bramwell, 1996). This fact and the simplicity of associated equivalent models make the implementation of the LGMD model in mobile robotic systems attractive.

There are only a few implementations using the LGMD model and associated properties in mobile robotic systems with reasonable performance. (Rind and Blanchard, 1996) implemented a very realistic version of the LGMD model. They concluded that the model in a complex environment could detect obstacles robustly but its behavior was very unpredictable.

In (Blanchard et al., 1999) it was used a mobile robot to study the proposed LGMD model in real environments. In their work the mobile robot could use proximity sensors or the LGMD model to avoid obstacles. When the proximity sensors were in use the LGMD model response was observed in search for clues.

In (Yue and Rind, 2005) was developed a system which tried to improve the LGMD model overall response. This system was implemented in a physical mobile robot with fairly good results. Their work concluded that this new system could allow the mobile robot to autonomously cruise an arena, filled

with blocks, without colliding, although further work was needed to further improve the system selectivity.

Yue et al. (2006) implemented the LGMD model in automobiles to detect possible collisions. The idea was to improve the performance of active security devices. Their work used genetic algorithms to best tune the model parameters. They concluded that more work was needed for a reliable collision detection system, specifically because during normal driving situations the system could flag false collision warnings.

The model has been continuing to evolve by adding new layers, normally based upon computer vision knowledge (Meng et al., 2009) (Stafford et al., 2007)

In this article, we are interested in understanding the LGMD model previously proposed by by (Yue, et al., 2006) and the achieved properties of the model versus the ones of the real neuron (Rind and Bramwell, 1996). The model is extensively studied when submitted to relevant simulated visual data sets. These studies enabled us to understand some of the model limitations and propose a new methodology to cope with them for obstacles detection and avoidance (Guest and Gray, 2006) (Rind, 2002). In our perspective, the new proposed method decreases the model complexity and increases the precision of obstacle detection.

The system performance is verified in an experiment in which a mobile robot equipped with a camera on its top, must autonomously navigate in a simulated environment. The obstacle detection algorithm is solely based in the LGMD model implemented in the robot.

The obtained results show the system robustness and reliability.

The LGMD neuron is only one example of a visual feature detector that acts fast and reliably. It can be used in the development of neuromorphic smart sensors, which do not give a measure but instead indicate or detect situations which demand motor actions. Steering action bases on perception is a requirement in this new era of robot that share their spaces with humans (Rind, 2002). Further, they are of outmost importance in the development of neuroprotheses for silicon retinas for instance.

## 2. LGMD MODEL

(Rind, 1996) proposed a model for the LGMD neuron circuitry. Due to the very complex nature of the initial model, other equivalent models were developed from the original one (see (Blanchard, et al., 2000), (Blanchard, et al., 1999), (Rind, 2002), (Yue, et al., 2006) and (Yue and Rind, 2005)) despite its complexity. Herein, we apply the LGMD model described in (Yue, et al., 2006). It is simpler compared to other available models, but the remaining properties are the required to achieve the project goals.

The model, depicted in figure 1, is divided in 3 group cells: photoreceptor (P), inhibition (I) and summing (S) layers and 2 single cells: the LGMD and feed-forward (FF) cell.

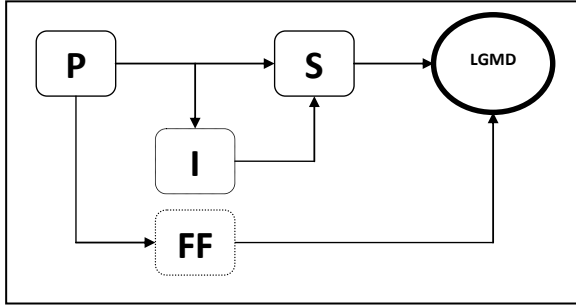


Fig. 1. LGMD model organization. Photoreceptor layer (P), Inhibition layer (I), Summing layer (S), LGMD cell and Feed-Forward cell (FF).

A grayscale image of the camera current field of view, represented has a matrix of color intensities, is the input to a matrix of photoreceptor units (P layer). This layer calculates the absolute difference between the luminance of the current and of the previous input images, that is:

$$P_f(x, y) = |L_f(x, y) - L_{f-1}(x, y)| \quad (1)$$

where  $P_f$  is the output of the P layer at frame  $f$  and  $L_f$  and  $L_{f-1}$  are respectively the captured luminance at frames  $f$  and  $f-1$ . The output of the P layer is the input of two layers: the inhibitory and the summing layer.

The inhibition layer (or I layer) receives the output of the P layer and applies a blur effect on it, using:

$$I_f(x, y) = \frac{1}{9} \sum_{i=-1}^1 \sum_{j=-1}^1 \delta(x+i, y+j), i, j \neq 0 \quad (2.1)$$

$$\delta(x, y) = P_f(x, y) + P_{f-1}(x, y) \quad (2.2)$$

where  $I_f$  is the output of the I layer at frame  $f$ , and  $P_f$  and  $P_{f-1}$  are the output of the P layer at frames  $f$  and  $f-1$ , respectively. Then, the output of the I layer passes, with one frame delay, to the summing layer.

The summing layer (or S layer) receives the output from the P and I layers and performs the following operation:

$$S_f(x, y) = P_f(x, y) - I_{strength} \cdot I_{f-1}(x, y), \quad S_f(x, y) \geq 0 \quad (3)$$

where  $P_f$  is the output of the P layer at frame  $f$ ,  $I_{f-1}$  the output of the I layer at frame  $f-1$  and  $I_{strength}$  (a scalar) the inhibition strength. The purpose of this operation is to remove the noise from the signal that comes from the P layer with the help of the I layer. The LGMD cell receives the output from the S layer and joins all the respective individual signals into only one signal:

$$LGMD(f) = \sum S_f \quad (4)$$

where  $LGMD(f)$  is the output of the LGMD cell at frame  $f$  and  $S_f$  is the output of the S layer, also, at frame  $f$ .

The feed-forward cell (FF cell) is a cell which is very similar to the LGMD cell but receives the output from the P layer (and not from the S layer), as follows:

$$FF(f) = \sum P_f \quad (5)$$

where  $FF(f)$  is the output of the FF cell at frame  $f$  and  $P_f$  is the output of the P layer, also, at frame  $f$ . The purpose the FF cell is to inhibit the LGMD layer when there are changes that include all the visual field.

## 3. MODEL ANALYSIS

Most important LGMD neuron model properties also present in the real LGMD neuron to present the simulations that confirm the properties on the LGMD neuron model. If discrepancies are found, these are justified.

Despite the importance of the presented results, these depend on the environment where the model is implemented/simulated. Results are mainly affected by the camera sampling frequency.

In fact these results are in accordance with the overall of results published so far (Rind and Bramwell, 1996), demonstrating the importance of the relative timing between excitation and inhibition for the selective response to approaching objects.

In this section, we present results when input video images are 100 (in horizontal) by 100 (in vertical) pixels; images were grey scale ranging from 0–255 (parameter without unit; similar parameters hereafter will not be restated). We generated image sequences simulating a camera with a field of view of 60° in both  $x$  and  $y$  axis with a sampling frequency of 10

Hz. The object being observed is a square black filled rectangle with dimensions as specified.

These results are obtained offline such that tests can be fairly compared since the network can be challenged with the same controlled visual images repeatedly.

The lateral inhibition spreads to its neighbor one layer away and with one frame delay. The local inhibition weight is 7.0. These parameters were tuned manually previously to the experiments and are kept constant throughout the article.

The LGMD-neural network model was written in Matlab (The MathWorks, Inc.). The computer used in this experiment is a Laptop (Toshiba Satellite L500-13W) with two 2 GHz CPUs (Intel Pentium Dual Core T4200) and Windows Vista Home Premium operating system.

#### a) Approaching Object

In these simulations a square object (20 x 20 cm), moves, on a direct collision course, from 100 cm up to 20 cm apart from the camera, with different but constant speeds of 0.1, 0.05, 0.025 and 0.0125 (m/s).

Results are depicted in Fig. 2. Each presented spike is the output of the LGMD cell (given by eq. 4), as calculated at each time step and plotted versus time.

A spike herein is not the LGMD pulse activity when the output of this cell exceeds a preset threshold as is usually done (Rind, 2002) (Yue et al, 2006).

Note that an object approaching with constant velocity has its edges moving with ever increasing speed (an increasing velocity of edge motion) and an increase of edge amount.

These results clearly show that, similarly to the LGMD neuron biological counterpart (Guest and Gray, 2006), as the object gets closer, the spiking activity is greater both in amplitude and frequency. It comes from the fact that as the object gets closer, its edges are bigger and move faster within the camera image than the lateral inhibition (Rind and Bramwell, 1996).

In survey, when object edges move at the frequency of the camera sampling time and the movement is greater than one pixel wide the results from the P layer only partially reach the S layer because it is still, in a small amount, affected by the I layer. Excitation in the model flows faster than the inhibition.

Decreasing the camera sampling frequency increases the speed of movement of the object edges, thus solving this specific problem. Another possibility is to tune the model parameters according to the object speed.

Blanchard et al. (2000) already pointed out that there was a need to tune the model's parameters for the speed of motion, when working in real, dynamic environments. This work enforces this need.

In the LGMD-model, the lateral inhibition underlies selectivity for objects rapidly approaching on a collision course. This selectivity depends on the critical race between the excitation and the laterally directed inhibition. Excitation dominates if it arrives before laterally extending inhibition and the LGMD network response builds up rapidly.

#### c) Lateral Movement (x and y axis)

The Locust LGMD neuron does not respond preferentially to one particular direction of constant motion in the X-Y plane, though it responds most strongly to large objects moving at high speeds.

The obtained results, depicted in Fig. 7 confirm these response properties, when an object 75 cm apart from the camera moves with a constant velocity (0.0125, 0.025, 0.05, 0.1 m/s) from 30 cm of one side of the camera to 30 cm in the opposite side.

These results show that, similarly to the LGMD neuron, as the speed increases only the number of spikes increase and the amplitude remains unchanged.

### 4. COLLISION AVOIDANCE SYSTEM

In this paper we evaluate the behavior of the LGMD network as a means to detect obstacles, when a robot relies only upon vision to extract information from

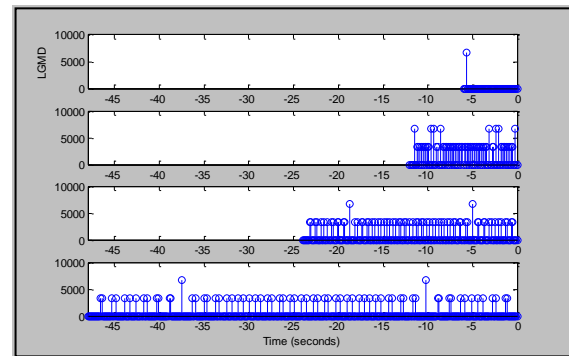


Fig. 7. LGMD model response when an object moves at constant distance (75 cm) from the camera with different velocities: 0.0125, 0.025, 0.05, 0.1 m/s.

the surrounding environment. We propose a LGMD-based collision avoidance system, similar to previous works (Blanchard et al., 2000), which have demonstrated the ability of an LGMD neural network to avoid collisions in an arena with both simple and more complex backgrounds.

In our experiments, a mobile robot surrounded by several obstacles (blocks), is expected to move without colliding with them. The LGMD-based collision detection system previously described was implemented in the mobile robot, and constitutes the

only mean of the robot to acquire sensory information, and as such avoid the blocks in the robot's path.

Experiments were done within a simulated environment, using the Webots (Michel, 2004) simulator. This is a simulation software based on ODE, an open source physics engine for simulating 3D rigid body dynamics.

The simulated environment is composed by a dark blue mobile robot surrounded by several red blocks, a yellow floor and a blue sky. The mobile robot is modeled as cylinder (22 cm radius and 62 cm height) with two wheels attached, working as differential wheels. It is also equipped with a CCD color camera (100 x 100 pixels) with a field-of-view of approximately 45°. This camera worked at 1 frame per second. The blocks are parallelepipeds with 30x30x60 cm in depth, width and height, respectively.

Initially, color images are captured by a CCD camera mounted on the top of the robot within the Webots (Michel, 2004) environment. This image is then converted to a grayscale image, with values in the discrete range from 0 to 255, which is then normalized to values in the continuous range of [0.0, 1.0].

The LGMD-based neural network previously described at section 2, is implemented in the Webots simulator and with the help of the OpenCV library. It takes the normalized image data from the camera and process it accordingly. The result is then sent to the Robot Controller, via a TCP/IP connection.

The Robot Controller module, implemented in MATLAB, receives spikes from the neural network and analyses them. This analysis decides the type of movement the robot will exhibit, either walking forward (straight) or turning. The resultant movement commands are sent via TCP/IP connection to the Robot module.

The Robot module controls the right and left wheels of the robot and outputs the necessary command values so that the robot behaves as decided.

#### 4.1. Robot Controller and Robot Module

The Robot is initially located in a spot, sufficiently apart from any block, and starts to move forward at a constant speed of 1 m/s. To move forward is achieved by a **walk command** which is sent to the Robot module that outputs equal velocities to both wheels. At each time step the LGMD spikes are received and averaged in an average window of 20 samples.

When the mean value of the LGMD model response is greater than a specified threshold (2000), an **evade command** is sent to the Robot Module instead. In this case, the robot is stopped and turned around its own axis. The turning speed is set to be  $-\frac{1}{3}$  m/s and

$\frac{1}{3}$  m/s for the left and right wheel, respectively. The robot thus turns left

During turning, the LGMD neural network output is not considered and is resettled to zero, such that the mean LGMD response starts to decay towards zero. It is necessary to suppress the LGMD network during rotations otherwise the sudden change in the visual scene would produce spikes that could cause false collision alerts.

When it reaches zero the robot is again commanded to move in a straight line. Therefore, the robot turning time is around 20 time steps.

## 5. SIMULATIONS

In order to verify the reliability of both the implemented LGMD model to obstacles detection and the proposed algorithm for obstacle avoidance, it is necessary to perform autonomous navigating experiments. Ideally, these should be verified in the real world. However, to simplify the problem we used firstly a simulated but physics-based environment, such that new and unpredictable situations are presented to the robot during its navigation.

Figure 8 depicts one experiment when the mobile robot moved autonomously during 13 s when surrounded by several obstacles (blocks). Four collisions were successfully detected by the LGMD-based collision detection system and 4 avoidances were performed.

First column depicts several snapshots of the experiment. Second column shows the corresponding time evolution of the LGMD model (blue "o" marker) and the LGMD mean (red solid line). The robot path up to the snapshots instant of time is depicted in the 3rd column. In the first column at every snapshot right upper corner, a picture shows what the robot "sees" at the instant of time depicted in the snapshot.

Initially, the robot is stopped and starts to move straight ahead (panel A in fig.17). As the robots starts to move the LGMD model spiking activity is high (panel B), having two gigantic spikes in the beginning.

To calculate the mean LGMD response the underlying algorithm needs 20 samples. So, before the 20th sample the mean LGMD response is zero (panel B). Once that happens, at  $t = 1.9$  s, instant corresponding to the snapshot depicted in panel A, the mean LGMD response immediately grows towards  $\approx 5000$ , a value larger than the specified threshold (2000) and an obstacle is considered to be detected. Then, the robot is commanded to evade.

One fact that stands out is that using the mean LGMD response instead of the raw LGMD response makes the obstacle detection algorithm simpler and immune to noise. This noise immunity can be

observed in both the LGMD response and its mean (Panels B, H, N, T). This robustness is especially important for real applications. Further, the proposed solution seems to improve the precision of the detection.

If we instead used algorithms based on detection of successive spikes, in which a spike is the LGMD pulse activity when the membrane potential exceeds a preset threshold, as usually done (Meng et al., 2009), (Yue et al., 2006), (Yue and Rind, 2005); detection would be made in very different occasions (depicted as a cyan spike in Panels B, H, N, T).

Note that the overall performance of the system would be very different. This performance increase can be verified by checking the distances to the blocks at the time of collision. At A the block was at 1.7 m. At G, M and S the block was at  $1.04 \pm 0.03$  m. This clearly demonstrates that precision of detection has increased. The difference in A is related to the fact that the system has just started working.

This is an innovative aspect of our approach compared to previous research (Meng et al., 2009), (Yue et al., 2006), (Yue and Rind, 2005).

In order to evade the obstacle, the robot starts to rotate. The LGMD response is not considered and is algorithmically truncated to zero, until the mean LGMD response decays to zero. The mean LGMD response decaying towards zero is shown in panel E. When it reaches zero (panel D), the robot is then commanded to move in a straight line. Further, the inhibition over the LGMD-network is released.

The robot starts again to move in a straight line as depicted in panel I. Note that the first three samples are truncated to zero (panel H). This is needed to avoid to take into account the noise created when the robot starts to move. After these first three samples, the LGMD response evolves (panel H) and when its mean grows higher than the specified threshold of 2000, an obstacle is detected. Therefore, at panel G, the robot is again commanded to evade.

Despite the fact that the LGMD response is slightly different for each time step, the robot continues to move autonomously within the environment, successfully avoiding the obstacles in its path.

In order to further verify the performance of the proposed LGMD-based obstacle system detection, we test the system under extreme conditions. Similar experiments are described by Yue (2006). The robot is faced with two scenarios, with a course duration of 23,4 s each: a) an extremely dark environment (luminance intensity of  $0.05 \text{ w/m}^2$ ); and b) an extremely light environment (luminance intensity of  $3.0 \text{ w/m}^2$ ). Experiments are depicted in Fig. 9. Under these extremely different light conditions, the system is still able to successfully avoid obstacles without additional difficulties (see figure 18, top and bottom).

This proves once again the robustness of the LGMD model.

## 6. CONCLUSIONS

In this article we verified the reliability of the LGMD neural network model by implementing it in a mobile robot within a realistic but simulated environment.

We have modified the model proposed in the literature to deal with some problems the robot was facing. The mobile robot was able to successfully avoid all the obstacles in its path and never colliding.

Also we show that by analysing the mean LGMD response instead of the raw LGMD response we improve the precision of the detection and noise immunity.

The LGMD model also revealed to work perfectly at very different lighting conditions. Further work includes the implementation of the model in a physical robot and the introduction of adaptability in the system parameters.

## ACKNOWLEDGMENTS

The authors would like to thank the FCT (“Fundação para a Ciência e Tecnologia”) by the support provided to this work.

## REFERENCES

- Blanchard, M., Rind, F.C. and Verschure, P.F.M.J. (2000). Collision avoidance using a model of the locust LGMD neuron.. *Robot Auton Syst* **30**, pp.17-38.
- Blanchard, M., Verschure, P.F.M.J. and Rind, F.C. (1999). Using a mobile robot to study locust collision avoidance responses. *International Journal of Neural Systems*, **9**, pp.405-410.
- Guest, B.B. and Gray J.R. (2006). Responses of a looming-sensitive neuron to compound and paired object approaches. *J Neurophysiol*, **95**, pp. 1428–1441.
- Meng, H., Yue, S., Hunter, A., Appiah, K., Hobden, M., Priestley, N., Hobden, P. and Pettit, C. (2009). A Modified Neural Network Model for Lobula Giant Movement Detector with Additional Depth Movement Feature. In: *IEEE International Joint Conference on Neural Networks*, June 14-29, 2009, Atlanta, Georgia.
- Michel, O. (2004). Webots: Professional mobile robot simulation. *International Journal of Advanced Robotic Systems*, **1**, pp.39–42.
- Rind, F.C. (2002). Motion Detectors in the Locust Visual System: From Biology to Robot Sensors. *Microscopy Research and Technique*, **56**, pp.256-269.
- Rind, F.C. and Bramwell, D.I. (1996). Neural network based on the input organisation of an identified neuron signalling impending collision, *J. Neurophysiol.*, **75**, pp.967–984.
- Stafford R., Santer R.D. and Rind F.C. (2007). A bio-inspired visual collision detection mechanism for cars: Combining insect inspired neurons to

create a robust system. *BioSystems*. **87**, pp.162-169.

Yue, S., Rind, F.C., Keil, M.S., Cuadri, J. and Stafford, R. (2006). A bio-inspired visual collision detection mechanism for cars: Optimisation of a model of a locust neuron to a novel environment. *Neurocomputing*, **69**, pp.1561-1598.

Yue, S. and Rind, F.C. (2005). A Collision Detection System for a Mobile Robot Inspired by the Locust Visual System. *Proc. IEEE Int. Conf. Robotics and Automation, Barcelona, Spain, Apr. 18-22*, pp. 2843-3848.

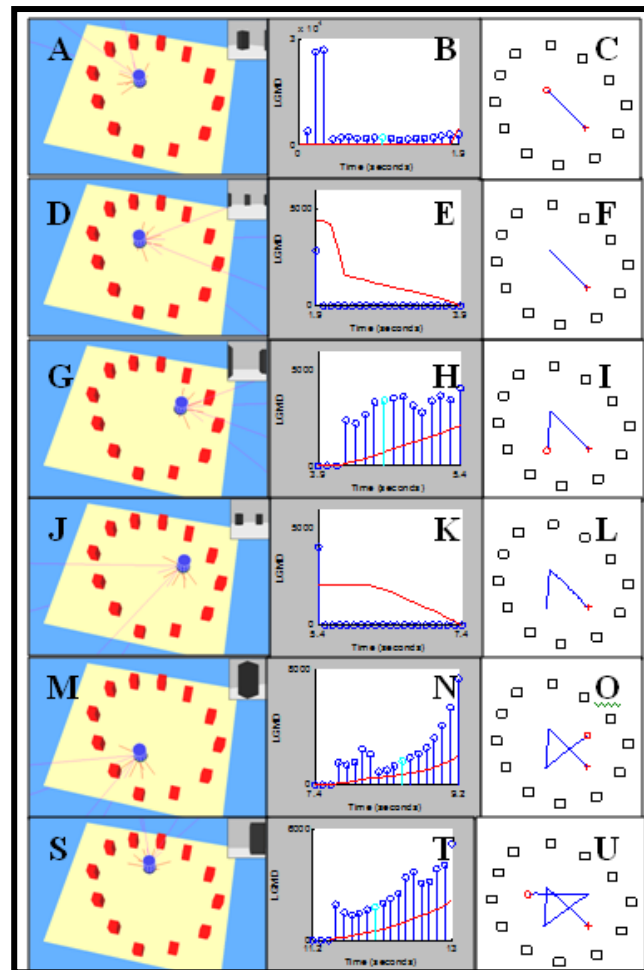


Fig. 8. Obstacle avoidance experiment results. Time increases from left to right, top to bottom. Each line represents different time steps of the experiment. First column: state of the environment at the end of each step. Second column: evolution of both the LGMD model output (in blue) and the mean LGMD model output (in red). Third column: Robot's path. The initial robot position is indicated by a cross.

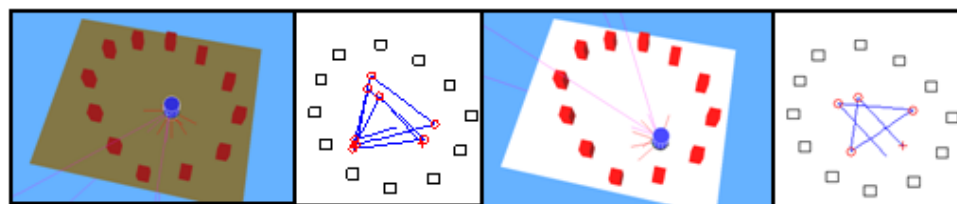


Fig. 9. Obstacle avoidance experiment for 23,4 s under two extreme different light conditions: Poor light conditions (0.05 w/m<sup>2</sup>) and very bright light conditions (3.0 w/m<sup>2</sup>). Snapshots of the environment and the robot path are shown. Robot speed is kept as before.